ИНСТИТУТ ЯДЕРНОЙ ФИЗИКИ
им. Г.И. Будкера СО РАН

Yu.N. Pestov, M.A. Tiunov

ELECTROSTATIC FIELD IN THE SPARK COUNTER WITH A LOCALIZED DISCHARGE

BudkerINP 94-77

НОВОСИБИРСК

Electrostatic Field in the Spark Counter with a Localized Discharge

Yu.N.Pestov and M.A.Tiunov

Budker Institute of Nuclear Physics
630090, Novosibirsk 90, Russia

ABSTRACT

This paper describes the results of detailed field calculations for a parallel-plate spark counter. The computer code SAM for two-dimensional geometries based on a solution of Bound Integral Equations by a collocation method was used. An accuracy of electric field calculations is 10^{-3}. Typical execution time for one electrode geometry is less than 60 s on a PC-486. This allowed us to optimize an electrode shape and estimate influence of defects at an electrode surface on electric field. The results of the calculations are important for a choice of a spark counter design and technology for spark counter mass production.

1 Introduction

A spark counter with a localized discharge (Pestov counter) [1] has been proposed as a base for the TOF system at the ALICE detector, CERN [2]. The time resolution of this TOF system should be at the level of $40 - 70$ ps, the total number of counter channels 170 000 at the total counter area about 150 m^2.

The spark counter consists of two parallel plate electrodes separated by a gas gap. A special gas mixture is used to absorb photons from a spark. To localize discharge after each spark at least one of the electrodes is manufactured from high resistive matter. A readout signal is induced by a spark on pads or strips placed on the back side of a high resistive electrode.

The time resolution of the spark counter improves with increasing of an electric field in the gap [3]. The time resolution of 25 ps was obtained at an electric field of about 600 kV/cm [4]. This value of the electric field is close to the experimental limit of an autoelectron emission from a cathode. Right choice of an electrode shape is important because any free electron injected from a cathode always produces a background spark.

Very high electric field could also appear on defects of electrode surfaces. Influence of electrode surface quality on the electrostatic field and ways of decreasing of defect influence on spark counter characteristics are discussed.

The electric field in the spark counter gap produces a high mechanical pressure, which could bend relatively thin electrodes and change electric field at some electrode regions. Different values of electric field produce different delay time of a breakdown relatively a detected particle. If the electric field in

the spark gap would be a constant with an accuracy of few percents all over a spark counter area, the full area time resolution would be practically equal to the local one [1]. To minimize the pressure effect of electric field spacers fixing the counter gap size are placed between electrodes but not out of the gap. Basing on the results of the field calculations and previous practical experience of work with the counters we compare different types of possible spacer designs.

The results of the electrostatic field calculations are discussed from the point of view a spark counter design and choice of a technology for mass production of spark counters.

2 Programming details

A description of the computer code SAM used for field calculations can be found in ref.[5]. This code for two-dimensional electrostatic problems is based on a solution of Bound Integral Equations (BIE) by a method of collocations with an aim to obtain surface charge distribution. In this method an effective charge density on an electrode surface is described by a cubic spline interpolation of charge density values in collocation points. As a result, the initial BIE are reduced to the system of linear equations for unknown values of the charge density in collocation points.

An important advantage of this program is a fast speed of calculations of the electric field strength on an electrode surface because it is just proportional to the surface charge distribution.

The high accuracy of calculations is achieved by an analytic separation of singularities of a BIE kernel in collocation points. For the same aim an analytic description of singularities of the electric field on electrode edges as well in places of contact of electrodes with dielectrics is used.

Special calculations showed that the calculation accuracy was limited by a value about 10^{-3}. This number is a result of an rough approximation of the electrode shape by a limited set of simple geometrical figures realized in SAM. A cone and a tore were used for an axial symmetric problem and a plane and a cylinder — in the case of a plane problem. However this accuracy is good enough for determination of an optimal geometry of the counter electrodes. Effective algorithms, realized in SAM allowed to produce all calculations on a IBM PC-486 computer. Typical execution time for one electrode geometry is less than 60 s.

3 Results

3.1 Choice of an electrode edge shape

An electrode edge shape must prevent from background discharges which could be initiated by increasing of the electric field. The well known Rogowski electrodes provide an almost homogeneous electric field in a central area between of two special shape disks, which decreases monotonously to the electrode edges [6].

In practice, unlike the Rogowski electrodes, spark counter electrodes should be plane on the whole and differ from a plane near their edges only. At this case the electric field always increases to edges but our task was to find an electrode shape, which provides permissible increasing of the electric field value.

Fig.1 shows a cross-section of half infinite spark counter electrodes by a plane, which is perpendicular to the electrode edge line. Beginning of a local $X-Y$-coordinate, connected with each electrode coincides with a point on the electrode cross-section where an electrode shape starts to deflect from the direct line. X-coordinate is a continuation of this line and directed to

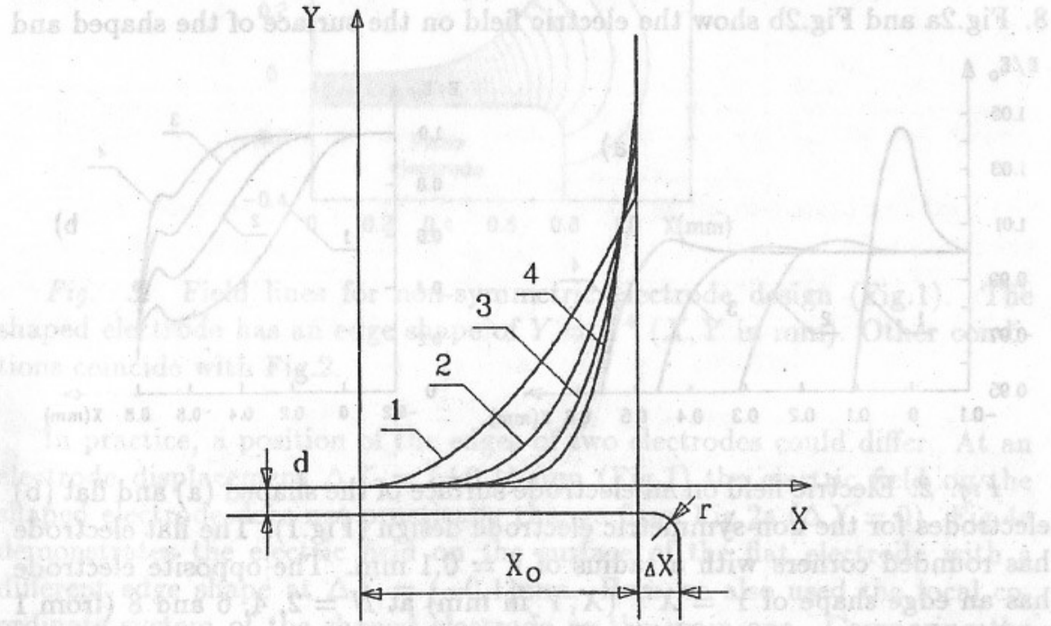

Fig. 1. Cross-section of the non-symmetric electrode design. The flat electrode and the opposite electrode with an edge shape of $Y = X^N$ (X, Y in mm) at $N = 2$, 4, 6 and 8 (from 1 to 4 in this figure, respectively) are shown.

an electrode edge. A direction of Y-coordinate is opposite to the gap side. An edge shape for the $X > 0$ was described by a formula

$$Y = X^N , \qquad (1)$$

where X and Y are the coordinates expressed in millimeters and N is a constant. Changing the N value we obtained different electrode edge shapes, which started from the beginning of a local $X - Y$-coordinate system and cross a point $X, Y = 1$ mm (Fig.1).

At the case of the non-symmetric electrode geometry one electrode was flat and the second one was shaped (Fig.1). At all calculations presented at this paper a thickness of electrodes was equal to 2 mm and a gap size — $d = 0.1$ mm. The flat electrode had rounded corners with a radius of $r = 0.1$ mm. A shape of the second electrode started to deflect from a direct line at a $X_0 = 0.8$ mm distance from the edge. This distance value is a result of performed calculations with an aim to minimize a dead area of the spark counter.

First calculation has been done for the identical position of the edges of both electrodes ($\Delta X = 0$, Fig.1). The electric field was calculated for an electrode edge shape given by a formula (1) with a N constant of 2, 4, 6 and 8. Fig.2a and Fig.2b show the electric field on the surface of the shaped and

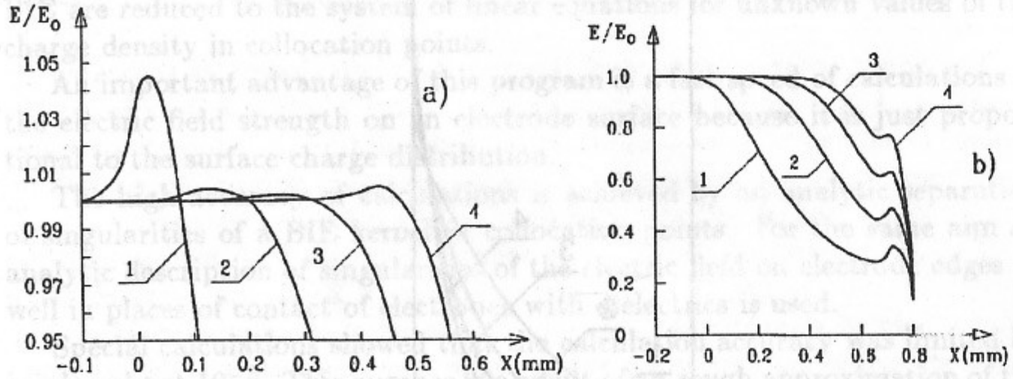

Fig. 2. Electric field on an electrode surface of the shaped (a) and flat (b) electrodes for the non-symmetric electrode design (Fig.1). The flat electrode has rounded corners with a radius of $r = 0.1$ mm. The opposite electrode has an edge shape of $Y = X^N$ (X, Y in mm) at $N = 2$, 4, 6 and 8 (from 1 to 4 in this figure, respectively). The electrode displacement of ΔX is equal to zero. A thickness of electrodes $D = 2$ mm and a gap size $d = 0.1$ mm. Beginning of a $X - Y$-coordinate is set at a distance of $X_0 = 0.8$ mm from the shaped electrode edge.

flat electrodes, respectively. Here we used the local coordinate system of the shaped electrode as the main one. The electric field on the shaped electrode surface has visible 5% increase as compared with the electric field in the gap (Fig.2a) for the edge shape (1) with $N = 2$. The electrode shape with $N = 4, 6$ and 8 provide electric field increase less then 1%.

Independently of the used shape of the opposite electrode the electric field on the flat electrode surface decreases from a maximum value inside the gap to a minimum one close to the edge and then increases slightly due to the influence of the corner of the flat electrode (Fig.2b). It is important that the electric field value on the surface of the flat electrode be everywhere less or equal to the gap field one.

Field lines for the electrode shape (1) with $N = 4$ are shown in Fig.3.

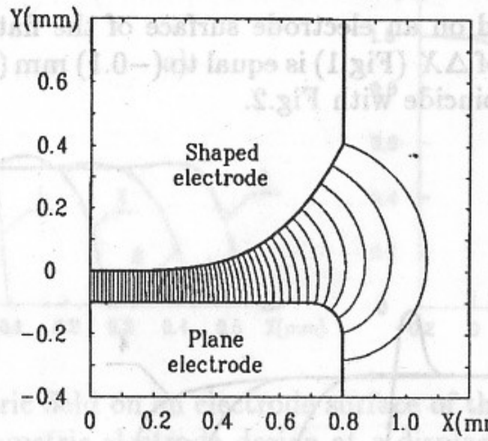

Fig. 3. Field lines for non-symmetric electrode design (Fig.1). The shaped electrode has an edge shape of $Y = X^4$ (X, Y in mm). Other conditions coincide with Fig.2.

In practice, a position of the edges of two electrodes could differ. At an electrode displacement $\Delta X = (\pm 0.1)$ mm (Fig.1) the electric field on the shaped electrode does not practically change from Fig.2a ($\Delta X = 0$). Fig.4a demonstrates the electric field on the surface of the flat electrode with a different edge shape at $\Delta X = (-0.1)$mm. Here we also used the local coordinate system of the shaped electrode as the main one. Comparing the results of this calculation with Fig.2b ($\Delta X = 0$) one can see that main changes of the field appeared near the corner of the flat electrode. However, the electric field value is still less than the electric field in the gap. For the electrode displacement $\Delta X = +0.1$ mm the field behavior near the corner of

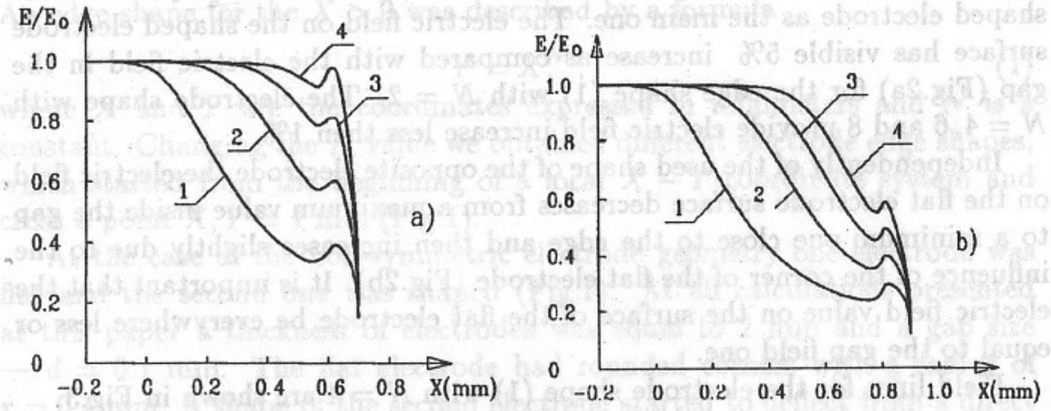

Fig. 4. Electric field on an electrode surface of the flat electrode. The electrode displacement of ΔX (Fig.1) is equal to (-0.1) mm (a) and $+0.1$ mm (b). Other conditions coincide with Fig.2.

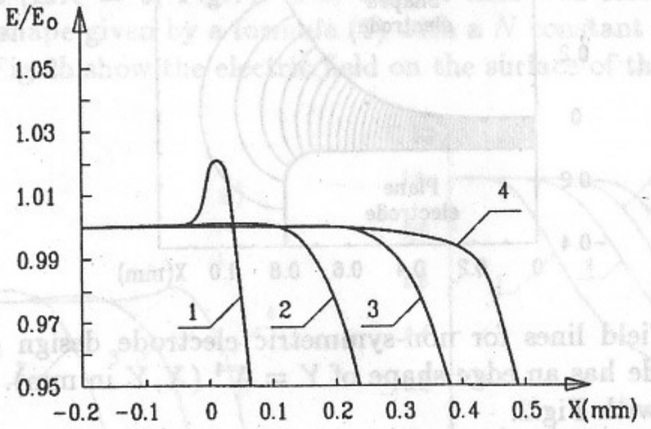

Fig. 5. Electric field on an electrode surface of the symmetric electrode design for an electrode edge shape of $Y = X^N$ (X, Y in mm) at $N = 2$, 4, 6 and 8 (from 1 to 4 in this figure, respectively). The electrode displacement is equal to zero. A thickness of electrodes $D = 2$ mm and a gap size $d = 0.1$ mm. Beginning of a $X - Y$-coordinate is set at a distance of $X_0 = 0.8$ mm from the electrode edge.

the flat electrode improved in comparison with the $\Delta X = 0$ case (Fig.4b).

Similar calculations of the electric field were done for the symmetric electrode geometry at the electrode shape (1) with N of 2, 4, 6 and 8 (Fig.5). The position of the edges of electrodes coincided at this case. For the electrode shape (1) with $N = 2$ increase at the level of 2.5% above a field value in the gap was obtained. For other types of the edge shape field increase is much less than 1% of the electric field value in the gap.

A relative displacement of the edge position of the electrodes by 0.1 mm changes the electric field on the surface of both electrodes making new field distributions quite similar to the distributions for the non-symmetric electrode geometry. Fig.6a shows the electric field on the surface of the electrode with the short edge. This distribution is similar to Fig.2a. The electric field on the surface of the long electrode decreases monotonously to the edge (Fig.6b) similar to Fig.4b. The main coordinate system coincides with the local one for the short electrode in this case.

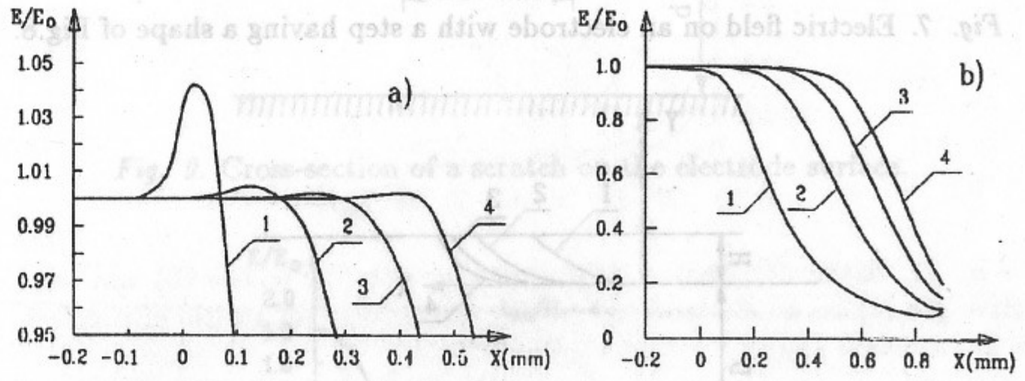

Fig. 6. Electric field on an electrode surface of the short (a) and long (b) edges of the symmetric electrode design at a displacement of edge electrode positions by 0.1 mm. The main coordinate system coincides with the local one for the short edge electrode. Other conditions are the same as in Fig.5.

3.2 Defects of the electrode surface

Defects on the electrode surface could be a source of high electric field. Defects with a size about the gap value of $d = 0.1$ mm could be locally shaped to decrease electric field. As one of examples we considered deflection from a set surface shape in the form of a step, which could be produced during manufacturing of electrode edges by a tool. Fig.7 shows the electric field distribution on the electrode surface for a step shape given by a formula (1) with a height of H=0.01 mm (Fig.8). For higher H values a field distribution near the shaped step practically coincides with the field near the counter edge (Fig.2a).

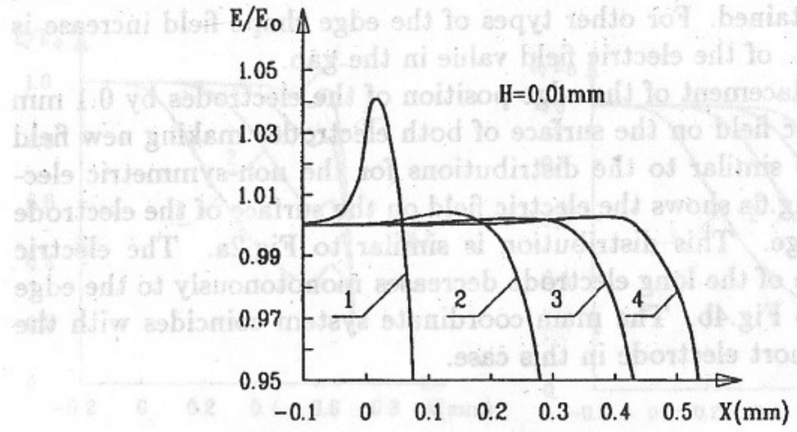

Fig. 7. Electric field on an electrode with a step having a shape of Fig.8.

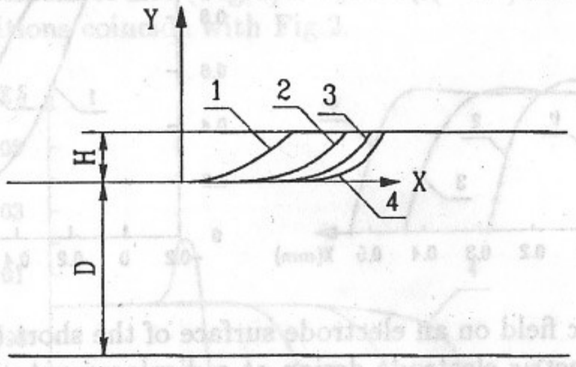

Fig. 8. Cross-section of a step on the electrode surface with an shape of $Y = X^N$ (X, Y in mm) at $N = 2$, 4, 6 and 8 (from 1 to 4 in this figure, respectively).

Casual single defects on an electrode surface with a size much less than the gap value of $d = 0.1$ mm could appear. They could be a result of an electrode matter structure, a method of surface treatment, polishing process or an evaporation of conductive matter on an electrode surface. Since the electric field depends on a surface shape of defects, the following calculations for one type of the defect shape should be considered as rough estimation of their influence on field. We calculated the electric field produced by a scratch, a hollow and a conductive pin on a flat surface of electrodes.

Fig.9 shows a shape of a scratch cross-section used for calculations. That is a smooth curve, having a depth H with respect to the electrode plane and

formed by four identical parts of a circle with a radius R. We supposed that a hollow is a cylindrical surface formed by the described above curve at an axis rotation coinciding with a symmetry axis of Fig.9. A pin cross-section has the same shape as a hollow but with a peak directed to the gap side.

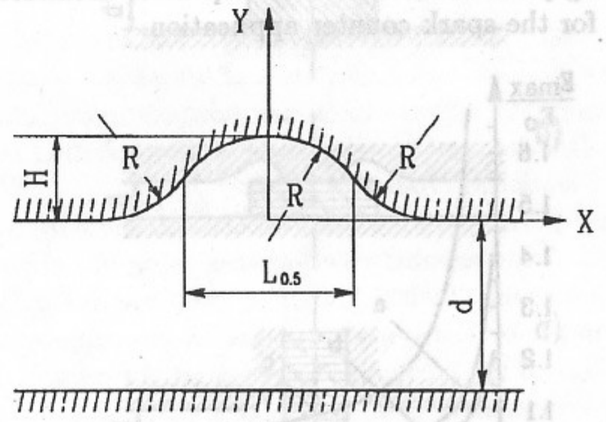

Fig. 9. Cross-section of a scratch on the electrode surface.

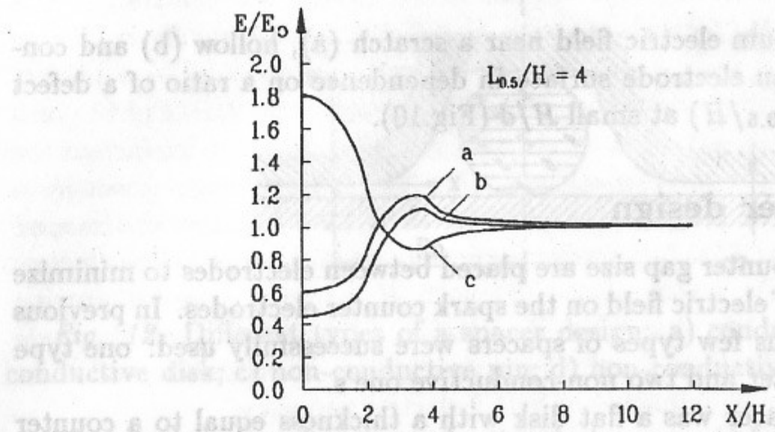

Fig. 10. Electric field near a scratch (a), a hollow (b) and a conductive pin (c) on an electrode surface.

Field distributions on a surface of an electrode with different types of defects are demonstrated in Fig.10. It is clear that a conductive pin is the most dangerous defect on an electrode surface. The calculations showed that field distributions do not practically depend on a scale of a defect (R/H=constant) if the height H of a defect is much less than the gap size $d = 0.1$ mm. So,

any sizes of small defects are equally dangerous. A maximum electric field value E_{max} of these distributions versus a ratio of a defect size to its height ($L_{0.5}/H$) is shown in Fig.11. Near a defect area, field increase of less than 5% is obtained for a $L_{0.5}/H$ ratio of 12 for a hollow, 20 for a scratch and 60 for a conducting pin. These numbers help us to estimate quality of the electrode surface for the spark counter application.

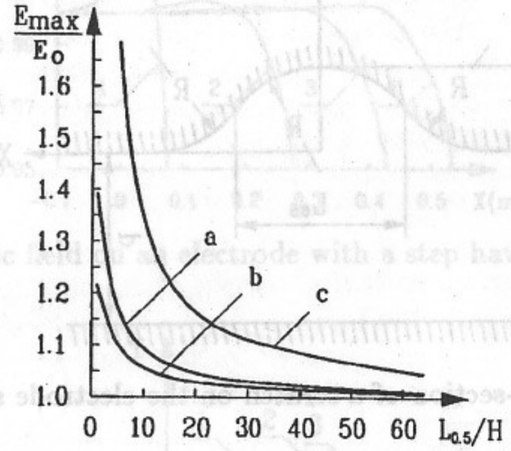

Fig. 11. Maximum electric field near a scratch (a), hollow (b) and conductive pin (c) on an electrode surface in dependence on a ratio of a defect size to its height ($L_{0.5}/H$) at small H/d (Fig.10).

3.3 New spacer design

Spacers fixing the counter gap size are placed between electrodes to minimize the pressure effect of electric field on the spark counter electrodes. In previous spark counter designs few types of spacers were successfully used: one type of a conductive spacer and two non-conductive one's.

A conductive spacer was a flat disk with a thickness equal to a counter gap size (Fig.12a) [7]. A direct current going through a spacer and a high resistive electrode decreased monotonously electric field from a maximum value up to zero near a spacer. This electric field behavior prevents from breakdown discharges near a spacer area.

The first type of a nonconductive spacer design was a flat non-conductive disk with a gap size thickness (Fig.12b) [8]. To prevent from breakdown discharges, at the semiconducting glass electrode just opposite the disk edge a circle groove was produced so that the electric field at this area was lower than the discharge threshold value.

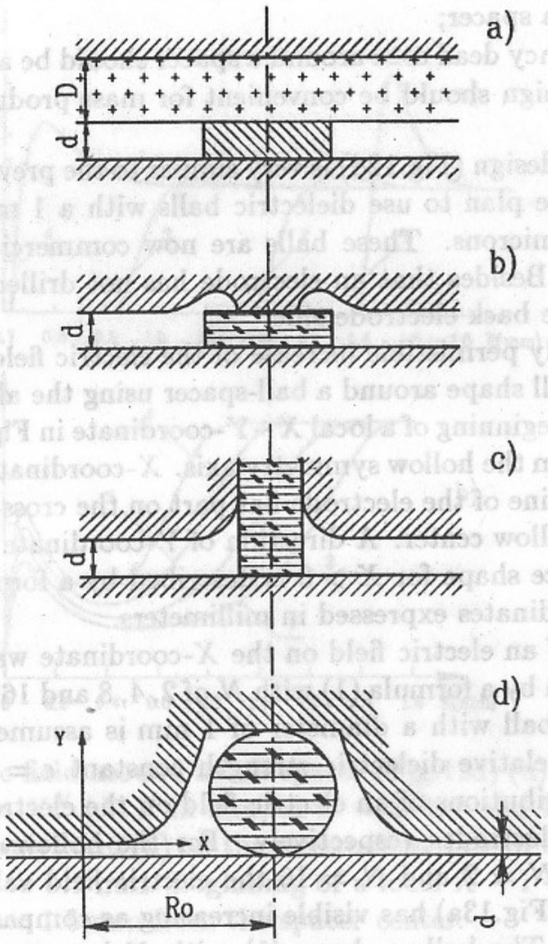

Fig. 12. Different types of a spacer design: a) conductive disk; b) non-conductive disk; c) non-conductive pin; d) non-conductive ball.

The second type of a nonconductive design was used at the spark counter prototype for the ALICE TOF system (Fig.12c) [4,9]. An insulating glass pin with a diameter of 1 mm was glued in a hole drilled in the semiconducting glass electrode. The pin height with respect to the electrode plane was equal to a counter gap size. A smooth hollow around a pin decreased electric field around a pin and prevented from background discharges along the pin surface.

In spite of the number of already used spacer designs we are not completely satisfied by them from point of view of a combination of next three criteria:

a) a design should provide only permissible increase of the electric field value near a spacer;
b) a low efficiency dead area around a spacer should be as small as possible;
c) a spacer design should be convenient for mass production and counter assembling.

A new spacer design (Fig.12d) is very similar to the previous one (Fig.12c). Instead of pins we plan to use dielectric balls with a 1 mm diameter at its accuracy of few microns. These balls are now commercially available at a cheap price [10]. Besides that an electrode has not drilled holes for spacers saving smooth the back electrode side.

To provide only permissible increase of the electric field near a spacer we chose a hollow wall shape around a ball-spacer using the algorithm described in a section 3.1. Beginning of a local $X-Y$-coordinate in Fig.12c is placed at a distance of R_0 from the hollow symmetry axis. X-coordinate is a continuation of the projection line of the electrode flat part on the cross-section plane and directed to the hollow center. A direction of Y-coordinate is opposite to the gap side. A surface shape for $X > 0$ is described by a formula (1), where X and Y is the coordinates expressed in millimeters.

Dependence of an electric field on the X-coordinate was calculated for a hollow shape given by a formula (1) with N of 2, 4, 8 and 16 and $R_0 = 1.5$ mm (see Fig.12c). A ball with a diameter of 1 mm is assumed to be a perfect insulator with a relative dielectric strength constant $\epsilon = 2.5$. Fig.13a and Fig.13b show distributions of an electric field on the electrode surface of the shaped and flat electrodes respectively. For the hollow shape given by a formula (1) with $N = 2$ and $N = 16$ the electric field value at the shaped electrode surface (Fig.13a) has visible increasing as compared to the electric field in the gap. The hollow shape (1) with N between 4 and 8 provide electric field increase less than 1%. The electric field on the plane electrode (Fig.13b) decreases from a maximum value to a minimum one and than increases slightly due to influence of ball dielectric property.

A low efficiency dead area around a spacer is defined by a ball diameter value of 1 mm and R_0 (Fig.12c), which could be minimized for each hollow shape. For an electrode shape (1) with $N = 4$ the R_0 value is equal to about 1.4 mm. Equal potential lines for an electrode shape (1) with $N = 4$ and $R_0 = 1.4$ mm are demonstrated in Fig.14. At these conditions Fig.15 shows the distribution of the electric field on the electrode surface of the shaped electrode. In the same figure the field distribution for the case of the conducting spacer design with a conductive disk diameter of 1 mm is shown. The new space design provides a dead area around spacer about 4 mm^2 that is much less than the 20 mm^2 dead area around a conductive disk spacer.

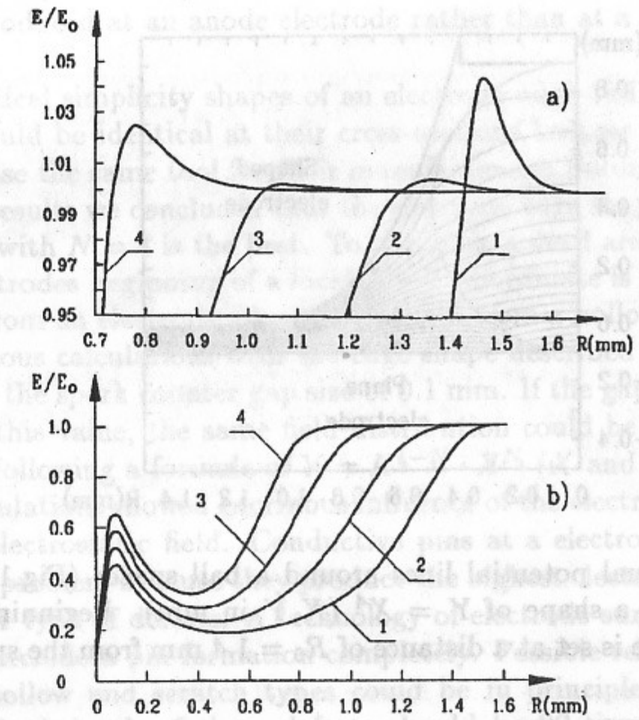

Fig. 13. Electric field around a ball spacer (Fig.12d) (a) on the electrode with a shape of $Y = X^N$ (X, Y in mm) at $N = 2$, 4, 8 and 16 (from 1 to 4 in this figure, respectively) and (b) on the electrode surface of the flat electrode. A gap size is equal to 0.1 mm. Beginning of a local $X - Y$-coordinate is set at a distance of $R_0 = 1.5$ mm from the spacer center.

4 Discussion

Let us first compare two types of an electrode geometry having symmetric and non-symmetric edge shape, which were investigated in section 3.1. An electric field distribution on the electrode surface for symmetric electrodes looks preferable (Fig.5). However a small electrode displacement of $\Delta X = 0.1$ mm makes these two geometries equivalent. From the point of view mass production accurate manufacturing of an electrode edge shape could be not simple. Small defects at edges could produce high electric field and following breakdown discharges. It was found experimentally that the spark counter is more sensitive to defects on a cathode than on an anode surface. That is understandable because any electron injected from a cathode always produces

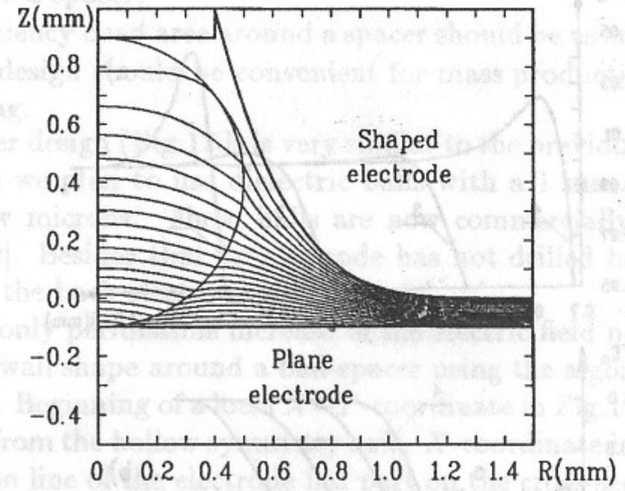

Fig. 14. Equal potential lines around a ball spacer (Fig.12d) with an electrode having a shape of $Y = X^4$ (X, Y in mm). Beginning of a local $X-Y$-coordinate is set at a distance of $R_0 = 1.4$ mm from the spacer center.

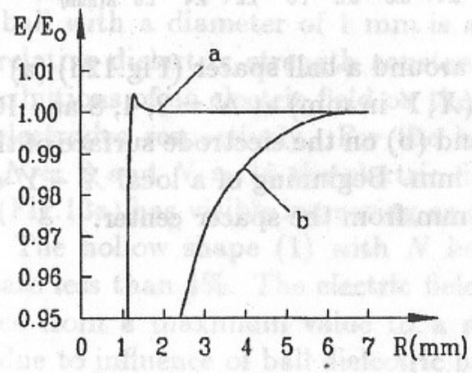

Fig. 15. Electric field (a) on the shaped electrode surface at a ball spacer (Fig.12d) and (b) around a conductive disk spacer with a diameter of 1 mm at a semiconducting electrode thickness of $D = 2$ mm (Fig.12a).

a spark. Initiation of a breakdown by a defect on an anode surface is a more complicated process [6].

Therefore at some conditions the spark counter design with a plane cathode and a shaped anode could be simple and practical. This conclusion concerns also the spacer design where a hollow around a non-conductive spacer should be produced at an anode electrode rather than at a cathode one (see section 3.3).

For practical simplicity shapes of an electrode edge and a hollow around a spacer should be identical at their cross-sections because at this case it is possible to use the same tool for their manufacturing. Summarizing previous calculation results we concluded that the electrode edge shape described by a formula (1) with $N = 4$ is the best. To minimize a dead area around shaped parts of electrodes beginning of a local $X-Y$-coordinate is put at a distance of 0.8 mm from an electrode edge and 1.4 mm from a hollow center.

All previous calculations with the edge shape described by a formula (1) are valid for the spark counter gap size of 0.1 mm. If the gap size differs in K times from this value, the same field distribution could be obtained for the edge shape following a formula of $Y = K^{1-N} \cdot X^N$ (X and Y – in mm).

The calculations showed enormous influence of the electrode surface quality on the electrostatic field. Conductive pins at a electrode surface is the most severe problem because they produce the highest electric field compared with another type of defects. A technology of electrode surface manufacturing should exclude a pin formation completely. Possible relatively large size defects of hollow and scratch types could be in principle smooth by polishing. A final depth of these defects should be 20 times less than their width. Calculation showed that even very small size defects could produce a high electric field. Most probably, experimentally obtained decrease of a background counting rate after first switching on a counter high voltage is a result of electrode surface treatment by sparks [1]. Of course this treatment could really influence on small size defects only due to a limited spark energy.

In section 3.3 different types of a spacer design were investigated from the point of view of an electric field distribution. These calculations and results of previous practical experience of work with the counters lead us to following conclusions. Disadvantages of the conductive spacer design are a large dead area and difficulties during a counter assembly procedure. A direct current through a spacer during counter operation is also undesirable. The design with a non-conductive disk has assembly problems. The design with a dielectric pin or ball type spacer has a small dead area of about 4 mm^2 and it is convenient for a counter assembly. We think that the new design with a dielectric ball spacer will be the simplest and cheapest one.

5 Summary

The main conclusions of this paper are:

1. Spark counter electrodes must be rounded near edges and nonconductive spacers to exclude breakdown discharges. A simple shape of an electrode surface at these areas has been proposed. An electrode surface should curve from a plane proportionally to a linear coordinate along a flat part electrode surface in a power of 4. Then increase of the electric field at these areas would be less than 1% of a field value in the gap.

2. The most simple and practical spark counter design should consist of a flat cathode electrode and a shaped anode one.

3. A technology for electrode manufacturing must exclude completely conductive pin defects on an electrode surface. Hollow type defects should be smooth with a ratio of their width to depth about 20.

4. A new convenient spacer design based on a dielectric ball has been proposed.

References

1. *V.V. Parhomchuck, Yu.N.Pestov and N.V.Petrovykh.* Nucl. Instr. and Meth. 93 (1971) 269.
   V.D.Laptev, Yu.N.Pestov and N.V.Petrovykh. Prib. Tekh. Eksp. 6 (1975) 36.
   A.D.Afanas'ev, V.D.Laptev, Yu.N.Pestov and B.P.Sannikov. Prib. Tekh. Eksp. 6 (1975) 39.
   Yu.N.Pestov and G.V.Fedotovich. Preprint INP 77-88, Novosibirsk (1977).
   V.D.Laptev, Yu.N.Pestov et al. Izv. AN SSSR, 42 (1978) 1488.
   Yu.N.Pestov, G.V.Fedotovich and K.N.Putilin. Proc. Int. Conf. on Instrumentation of Colliding Beam Physics, SLAC-250 UC-34D (1982) 127.
   Yu.N.Pestov. Proc. Int. Conf. on Instrumentation of Colliding Beam Physics, INF, Novosibirsk (1984) 163.
   A.Ogawa, W.B.Atwood, N.Fujiwara, Yu.N.Pestov and R.Sugahara. IEEE TRAS. NUCL. SCI. NS-31, 1 (1984) 121.
   N.Fujiwara, A.Ogawa, Yu.N.Pestov and R.Sugahara. Nucl. Instr. and Meth. NIM A240 (1985) 275.
2. Letter of Intent for ALICE, CERN/LNCC/93-16, 1993.

3. *Yu.N.Pestov.* Nucl. Instr. and Meth. A265 (1988) 150–156.
4. *Yu.N.Pestov.* Exper. Apparatus for High Energy Particle Physics and Astrophysics, 4th San Miniato Topical Seminar, World Sientific, (1991), 156.
5. *M.A.Tiunov, B.M.Fomel and V.P.Yakovlev.* Preprint INP 89-159, Novosibirsk, 1989.
6. *J.M.Meek and J.D.Craggs J.D.* Electrical Breakdown in Gases, Oxford, 1953.
7. *W.B.Attwood, G.B.Bowden, G.R.Bonneaud et al.* Nucl. Instr. and Meth. A206 (1983) 99–106.
8. *I.B.Vasserman, P.M.Ivanov, Yu.N.Pestov et al.* Jadernaja Fizica 28 (1978) 968; Jadernaja Fizica 33 (1981) 709.
9. *H.R.Schmidt.* TOF, Internal Note ALICE 93-36, November 1993.
10. *H. Gaizer and H.R.Schmidt.* Private communication.

Yu.N. Pestov, M.A. Tiunov

Electrostatic Field in the Spark Counter with a Localized Discharge

Ю.Н. Пестов, М.А. Тиунов

Электрические поля в искровом счетчике с локализованным разрядом

BudkerINP 94-77

Ответственный за выпуск С.Г. Попов
Работа поступила 18 мая 1994 г.

Сдано в набор 13.09. 1994 г.
Подписано в печать 13.09 1994 г.
Формат бумаги 60×90 1/16 Объем 1,8 печ.л., 1,5 уч.-изд.л.
Тираж 200 экз. Бесплатно. Заказ N 77

Обработано на IBM PC и отпечатано на
ротапринте ИЯФ им. Г.И. Будкера СО РАН,
Новосибирск, 630090, пр. академика Лаврентьева, 11.